Effect of Dynamic Yield Strength of Circular Saw Blade on Laser Shock Tensioning Process

Bo Li* and Zhankuan Zhang

A laser shock tensioning process is proposed in this work for circular saw blades. To explore the tensioning stress formation mechanism of the laser shock tensioning process, a theoretical model was built based on a finite element method utilizing reasonable simplifications and assumptions. By comparing theoretical analysis and the measured results, the theoretical model proved to be correct and the laser shock tensioning process proved feasible. The effect of the dynamic yield strength of the circular saw blades on the laser shock tensioning process was studied. Simulation results showed that the dynamic yield strength of the circular saw blades exhibited a strong effect on the overall tensioning. Circular saw blades with a higher dynamic yield strength can obtain greater room for improvement *via* the tensioning effect.

Keywords: Finite element method; Circular saw blade; Tensioning; Stress; Laser shock

*Contact information: Research Institute of Wood Industry, Chinese Academy of Forestry, Beijing 100091, China; *Corresponding author: libohongxing@sina.com*

INTRODUCTION

A circular saw blade is an important and widely used tool for the wood industry. Its stability, cutting precision, and material-saving abilities are the most important features, especially for the wood processing industry because of the shortage of high-valued wood (Li *et al.* 2015a). In recent years, the Chinese government has strongly supported the improvement of timber utilization, which promotes the development of circular saw blade manufacturing technology in China.

When a circular saw blade is cutting a workpiece, tangential and radial tensile stresses are produced due to the high rotational speed of the blade. These two kinds of stress cause no harm for the circular saw blade at work. However, thermal stress is also produced because the temperature at the edge of the blade is higher than other regions. This causes large tangential compressive stress at the edge of the circular saw blade, causing buckling deformation that reduces cutting precision, increases kerf loss, and shortens the saw life (Li *et al.* 2015b).

Plastic deformation in local areas of the circular saw blade is produced by mechanical or physical means, and tangential tensile stress at the edge of the circular saw blade is produced to compensate for the tangential compressive stress caused by thermal stress. This process is called tensioning, and it is the most important process for circular saw blades and can determine the quality of the saw blade. Li *et al.* (2016) pointed out that the tensioning stress field has the greatest impact on dynamic stability of a saw blade.

Hammering and rolling are the most widely used tensioning processes. But they have some disadvantages in terms of the tensioning effect, efficiency, and automation, which limit the development of tensioning processes.

The tensioning stress field of tensioned circular saw blades has been studied by many scientists based on theoretical methods and experimental means. The tensioning stresses of roll tensioned circular saw blades were tested, and their effects on the stability of the circular saw blade were discussed (Szymani and Mote 1974). The tensioning stress fields of roll tensioned circular saw blades were obtained based on experimental measurements and theoretical analysis (Szymani and Mote 1979). A theoretical model was presented that could accurately describe the tensioning stress field in a roll tensioned circular saw blade (Schajer and Mote 1983). A mathematical model that allows the prediction of optimal tensioning parameters for a saw blade was built (Schajer and Mote 1984). An X-ray stress test method was studied for measuring the tensioning stress field of roll tensioned circular saw blades (Umetsu 1989). Umetsu *et al.* (1994) measured the tensioning stresses in circular saw blades after hammering *via* an X-ray stress meter. Nicoletti *et al.* (1996) built a finite element model for roll tensioning processes and calculated the tensioning stress field. The effects of roll tensioning parameters on the tensioning stress field were examined using ABAQUS software (Heisel *et al.* 2014). The effect of yield strength on the tensioning stress field of the roll tensioned circular saw blade was studied (Li and Zhang 2017).

Laser shock peening (LSP) can significantly improve the fatigue performance of metallic components by forming a considerable residual compressive stress, and grain refinement can occur on the surface of the metal *via* the action of the laser shock wave (Huang *et al.* 2013). Plastic deformation is produced during LSP, which is the common ground with the tensioning processes. Laser shock peening is widely used in aerospace, the nuclear industry, and other fields (Cuellar *et al.* 2012). It also, has an incredible advantage in efficiency, accuracy, and automation (Achintha *et al.* 2014), which can play a great role in the field of tensioning processes. Currently, most scholars focus on compressive stress produced by a laser shock peening process and the research results are mainly used to improve the fatigue life of metal parts. There has been no research about the application of tensile stress produced by laser shock.

For the tensioning processes, the generation and precise control of the tensioning stress fields is an important issue in science and technology. Therefore, this paper proposes a laser shock tensioning process for using the advantages of LSP that can account for the deficiency of the existing tensioning technology.

Dynamic yield strength is the main performance parameter for a circular saw blade. In this paper, the effect of dynamic yield strength of circular saw blade on laser shock tensioning process was analyzed. The results of this research can be used to promote the application of laser shock tensioning process of circular saw blades with high strength.

EXPERIMENTAL

Materials

The circular saw blade was made from alloy spring steel GB 65Mn. Its hardness was HRC 42 and its dynamic yield strength was 1.29 GPa. Its external diameter, center bore diameter, and thickness were 220 mm, 30 mm, and 2.2 mm, respectively. The circular saw blade was manufactured in the Tianjin Forestry Tools Factory (Tianjin, China).

The parameters of the laser shock tensioning process are shown below. A Nd: YAG pump laser was used (Beamtech Optronics Co., Ltd., Beijing, China). The laser energy was 30 J, the spot diameter was 3 mm, the laser pulse width was 20 ns, and the radius of impact

zone was 6 mm. The laser parameters were used for the calculation of laser shock wave peak pressure. The thickness of running deionized water (confining layer) was approximately 1 mm. The thickness of the aluminum film (absorption protective layer) attached to the surface of the circular saw blade was 100 μm. The laser shock and related equipment were supplied by the Research Institute of Aviation Engineering (Beijing, China). The impact zone and laser spot distribution for the laser shock tensioning process are shown in Fig. 1. The overlap ratio between laser spots was as small as possible.

Many discrete local regions are impacted by laser and plastic deformations are produced in these regions. Tangential tensile stress will be produced in the edge of circular saw blade, which can compensate for the tangential compressive stress caused by thermal stress. That is the main feature of laser shock tensioning process. Laser shock tensioning process is the intersection and integration of laser shock peening and tensioning process.

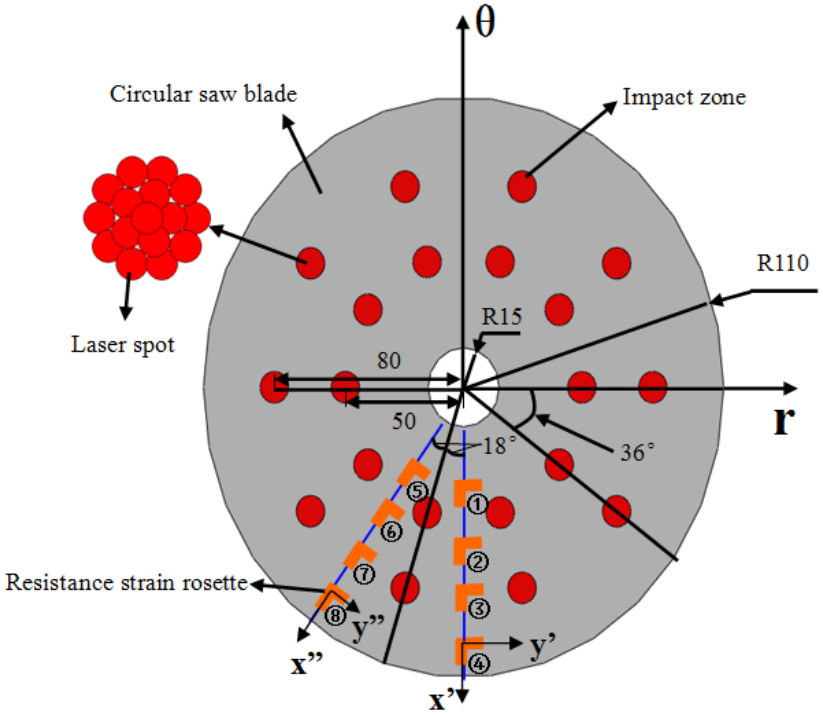

Fig. 1. Impact zone distribution of laser shock tensioning process

Methods

Tensioning stress

The double side of the circular saw blade can be loaded synchronously during a laser shock tensioning process. However, because of limitations of experimental conditions, one end surface of the circular saw blade was first shocked by the laser and the corresponding region of the other end surface was shocked by the laser later in the experiment.

Resistance strain rosettes (two axis, 90°) were attached to the surface of the circular saw blade, with waterproof and heat insulation treatments, as shown in Fig. 1. The resistance strain rosettes (Yiyang Strain and Vibration Testing Technology Co., Ltd., Beijing, China) were connected to a static strain acquisition instrument (Yiyang Strain and Vibration Testing Technology Co., Ltd., Beijing, China) until the end of the laser shock tensioning process. The strain of the final state was recorded *via* computer. Experimental pictures are shown in Fig. 2.

For the resistance strain rosettes 1 through 8, tensioning stress can be described as shown in Eq. 1,

$$\varepsilon_r = \varepsilon_{0°}$$
$$\varepsilon_0 = \varepsilon_{90°}$$
$$\sigma_r = \frac{E\left(\varepsilon_r + \mu\varepsilon_0\right)}{1-\mu^2} \quad (1)$$
$$\sigma_\theta = \frac{E\left(\mu\varepsilon_r + \varepsilon_\theta\right)}{1-\mu^2}$$

where, $\varepsilon_{0°}$ and $\varepsilon_{90°}$ are the strain of the resistance strain rosettes (°), ε_r and ε_θ are the radial and tangential strain (dimensionless), ε_r and ε_θ are the radial and tangential stress (MPa), E is the elastic modulus of the circular saw blade (210 GPa), and μ is Poisson's ratio of the circular saw blade (0.3).

The $\varepsilon_{0°}$ and $\varepsilon_{90°}$ of points 1 through 8 of the circular saw blades in the final state were tested *via* the resistance strain rosette.

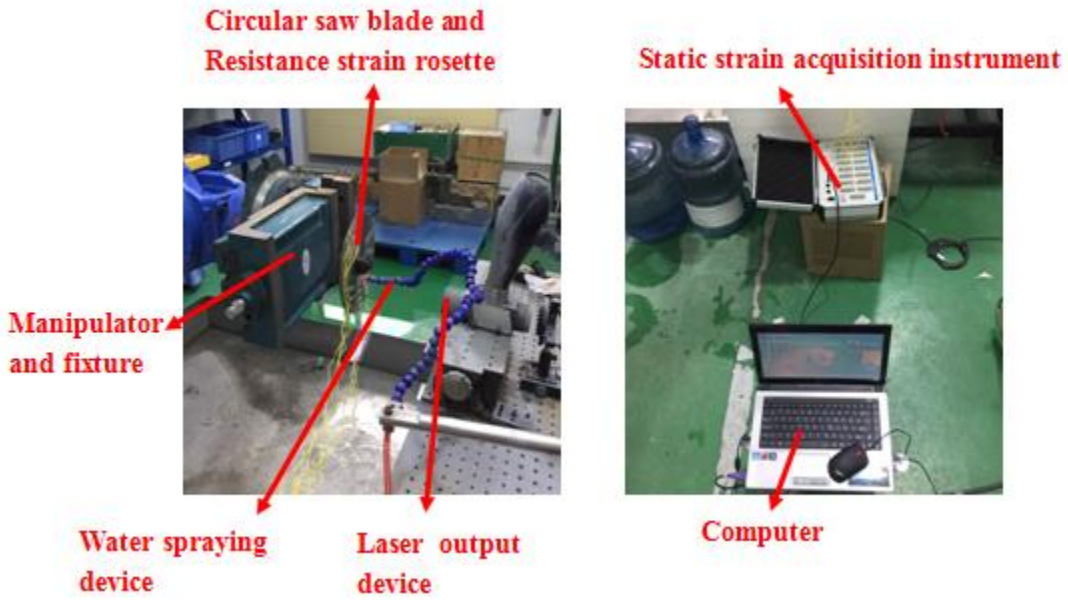

Fig. 2. Pictures of the equipment used in the experiments

MODELLING

Theoretical Calculation of Peak Pressure of Shock Wave

The peak P_{max} pressure of the laser shock wave was given as Eq. 2 (Ding and Ye 2006),

$$P_{max} = 0.01\left(\frac{\alpha}{2\alpha+3}\right)^{0.5} Z^{0.5} I_0^{0.5} \quad (2)$$

where α is the efficiency of the interaction. It is also reasonably assumed that 10% (α = 0.1) of the incident energy density is used for the pressure rise of the plasma (Peyre *et al.*

1996), Z is the reduced acoustic impedance (g.cm^{-2}.s^{-1}), and I_0 is the laser power density (GW/cm^2).

The laser power density, I_0, is expressed as shown below in Eq. 3,

$$I_0 = \frac{4E}{\pi d^2 \tau} \quad (3)$$

where E is the laser energy (J), d is the laser spot diameter (mm), and τ is the laser pulse width (ns).

The reduced acoustic impedance, Z (g.cm^{-2}.s^{-1}), is expressed according to Eq. 4,

$$Z = 2\frac{Z_{target} Z_{water}}{Z_{target} + Z_{water}} \quad (4)$$

where Z_{water} is the acoustic impedance of water (g.cm^{-2}.s^{-1}), $Z_{water} = 0.165 \times 10^6$ g.cm^{-2}.s^{-1}, Z_{target} is the acoustic impedance of steel (g.cm^{-2}.s^{-1}), $Z_{target} = \rho D$ (g.cm^{-2}.s^{-1}), ρ is the density of steel (ρ = 7.8 g.cm^{-3}), D is the shock wave velocity (D = 5200 cm.s^{-1}), and $Z_{target} = 4.056 \times 10^6$ g.cm^{-2}.s^{-1}.

In the experiment, E = 30 J, d = 3 mm, and τ = 20 ns. The peak pressure of one laser spot, P_{max}, calculated by Eqs. 2 through 4, was 4.58 GPa. The P_{max} was introduced into the theoretical analysis model for its verification.

Simplified Mechanical Model for Laser Shock Tensioning Process

The laser shock tensioning process is a complicated nonlinear mechanical process. The directly three-dimensional simulation of laser shock tensioning process by finite element method needs a large number of elements. Very low computational efficiency hinders the simulation and exploration for this process. Therefore, three assumptions were made to establish its theoretical model, as shown below.

The impact zone is joined by a number of laser spots in order to improve the tensioning effect, as shown in Fig. 3. The laser spot only plays the role of extending the impact zone. Therefore, the overlap ratio between laser spots is kept as small as possible. Although the outer edge of actual impact zone is not the ideal circle and the actual impact zone area is slightly smaller than circular area, the small overlap region of laser spots can compensate for this difference to some extent. Therefore, situations 1 and 2 in Fig. 3 were approximately equivalent and had the same shock wave peak pressure, which has scientific support and engineering significance.

The plastic deformation of the different impact zones was assumed to be the same, and the effect between these different impact zones was not considered due to its minute influence.

The impact zone of the circular saw blades was replaced by a through-hole. The inner wall of the through-hole was subjected to equivalent radial stress, as shown in Figs. 3 and 4. The stress field obtained by the abovementioned model was approximately equivalent to the tensioning stress field.

An axially symmetrical model was built to simulate one impact zone laser shock process using ABAQUS software (version 6.10, Dassault SIMULIA, Providence, RI, USA). Its loading process was simulated by a Dynamic/Explicit solution module. The step time was set to 7000 ns. Its unloading process was simulated by a Static/General solution module using the stress field of the loading process as the initial conditions.

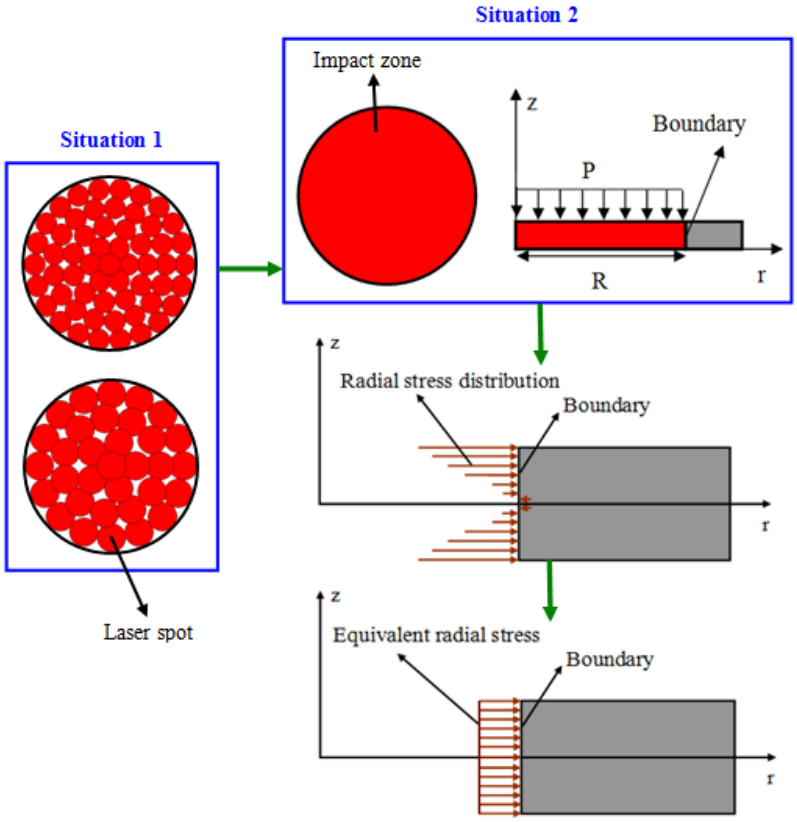

Fig. 3. Simplification of the mechanical model of the laser shock tensioning process

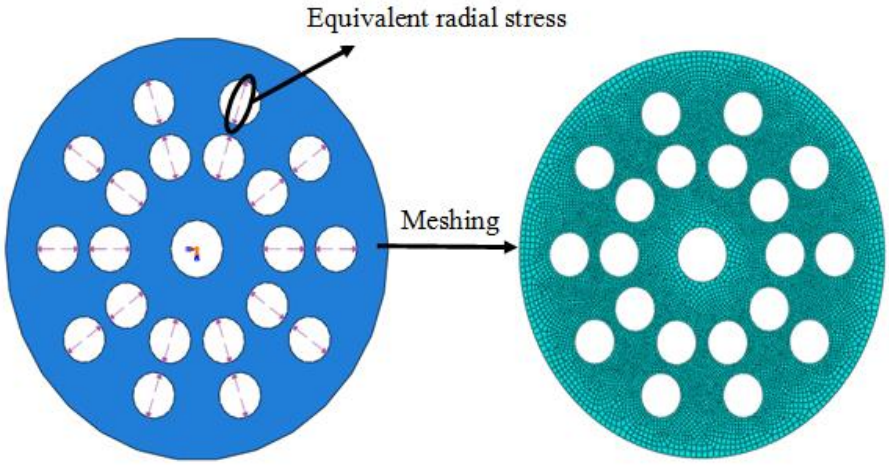

Fig. 4. Mechanical model of the circular saw blade with through-holes

The thickness of the circular saw blade was 2.2 mm. Many scholars have built theoretical models of the laser shock peening process using ideal elastic-plastic model. The model has been shown to be very close to the real situation (Luo *et al.* 2015; Hfaiedh *et al.* 2015; Hu *et al.* 2006; Dai *et al.* 2014; Braisted and Brockman 1999; Hua *et al.* 2010). Therefore, the material model of the circular saw blade was set as an ideal elastic-plastic model. The dynamic yield strength for the circular saw blades were set as 1000 MPa, 1290 MPa, 1500 MPa, 2000 MPa, and 2500 MPa for analysis and verification. Poisson's ratio for the circular saw blade was set as 0.3. Its elastic modulus and density were set as 210 GPa and 7.8 g/cm^3, respectively.

Symmetry constraint in the z direction was applied to the symmetry plane in the thickness direction of the circular saw blade, as shown in Fig. 5. The shock wave pressure load was applied to the impact zone. The shock wave peak pressure was set as 4.58 GPa first for establishing the correctness of the theoretical model. No matter what the laser parameters are, the peak pressure of laser shock wave is the final result. Therefore, the shock wave peak pressure was set as 2 GPa to 14 GPa, which was used for analyzing the tensioning effect of circular saw blade under different load. The curve of the shock wave pressure *versus* time is shown in Fig. 5. The 4-node bilinear axisymmetric quadrilateral element CAX4R was chosen for the circular saw blade.

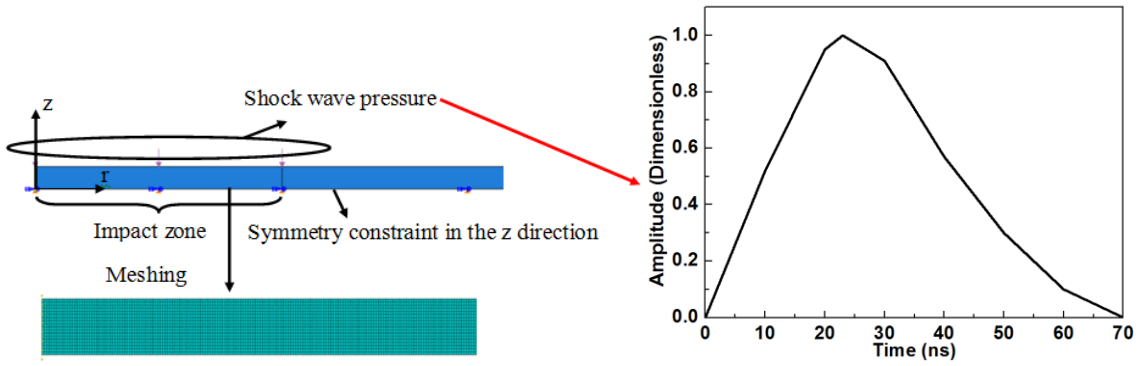

Fig. 5. Finite element model for one impact zone laser shock process

A plane stress finite element model was built, as shown in Fig. 4. A displacement fixed constraint was applied to the inner wall of the center hole of the circular saw blade. The equivalent radial stress applied to the inner wall of the through-hole was obtained by the finite element model as shown in Fig. 5. The radius of the through-holes (radius of impact zone) was set as 6 mm, 8 mm, 10 mm, and 12 mm. The 4-node bilinear plane stress quadrilateral element CPS4R was chosen for the circular saw blade.

RESULTS AND DISCUSSION

The results, shown in Figs. 6 and 7, were based on the experimental conditions. The shock wave peak pressure was 4.58 GPa.

As shown in Fig. 6, along the center of circular saw blade, the tensioning stress field of the elastic deformation region outside the impact zones had a cyclic axisymmetric distribution. This shows that the tensioning stress inside the circular saw blade was relatively uniform. Maximum and minimum tangential tensile stresses at the outer edge of the circular saw blade were marked as shown in Fig. 6.

Measured tensioning stresses were extracted from the positions in Fig. 1. Simulated tensioning stresses were extracted from the path in Fig. 6. As shown in Fig. 7, the simulation results were comparable to the experimental results. It is noteworthy that the tangential tensile stress was produced at the edge of the circular saw blade after the laser shock tensioning process, which is an important sign of the tensioning effect. Meanwhile, the tangential tensile stress increased with the radius in the edge of the circular saw blade, which was a favorable distribution form. The distribution form of the plastic deformation zones determines the distribution of the tensioning stress (Li *et al.* 2015a, 2015b). The experimental results not only established the correctness of the simulation model, but it

also illustrated the feasibility of the laser shock tensioning process. Although the laser shock tensioning process has not yet been applied, the research results of this paper are important technical reserves for future promotion of this technology.

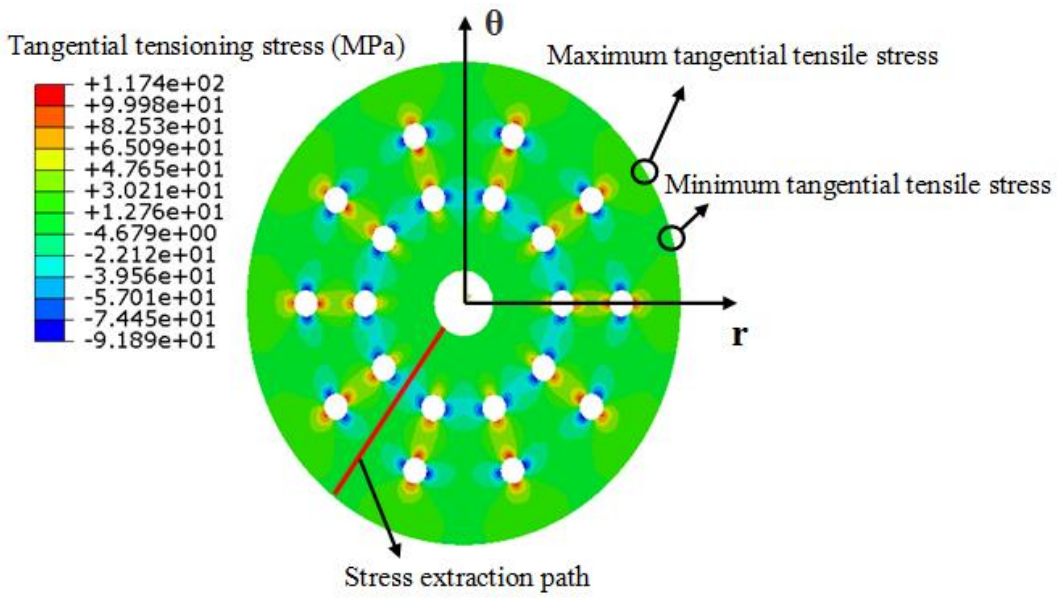

Fig. 6. Tangential tensioning stress field of the circular saw blade after the laser shock tensioning process

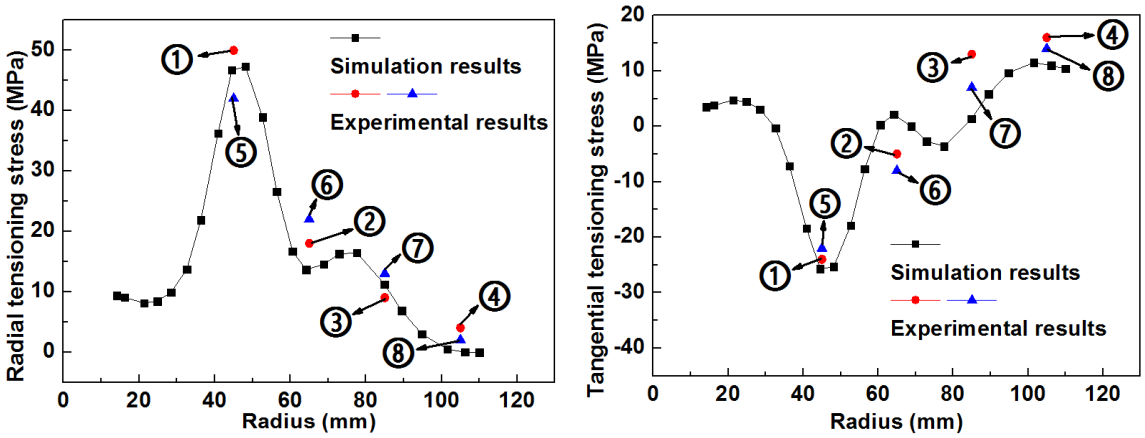

(a) Radial stress distribution (b) Tangential stress distribution

Fig. 7. Contrast of the tensioning stresses between simulation and experimental result

The average tangential tensile stress at the outer edge of the circular saw blade is the focus of this article. It is an important indicator for the laser shock tensioning process on the circular saw blade. Equivalent radial stress and the impact zone radius all had an effect on the average tangential tensile stress at the outer edge of the circular saw blade. As shown in Fig. 8, the average tangential tensile stress at the outer edge of the circular saw blade increased with the equivalent radial stress and the impact zone radius. This meant that the tensioning effect improved *via* increased equivalent radial stress and impact zone radius.

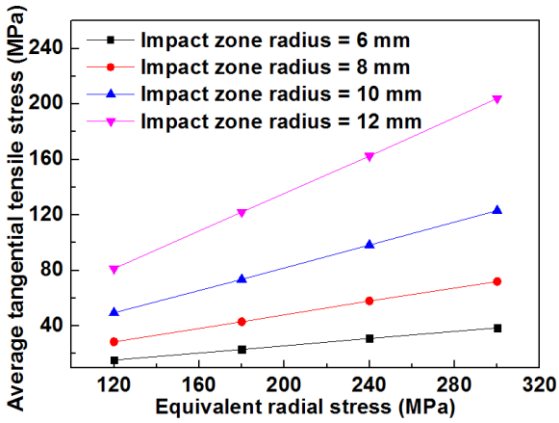

Fig. 8. Relationship between the average tangential tensile stress, equivalent radial stress, and impact zone radius

The impact zone radius had no effect on the equivalent radial stress. However, the dynamic yield strength of the circular saw blade had a strong effect on the equivalent radial stress. The effect of the dynamic yield strength on the tensioning effect was mainly reflected in its effect on the equivalent radial stress, which is discussed with emphasis as shown below.

The relationship between dynamic yield strength σ_y^D and Hugonoit elastic limit (HEL) is shown in Eq. 5 (Luo *et al.* 2015; Hfaiedh *et al.* 2015),

$$\sigma_y^D = HEL\frac{1-2\nu}{1-\nu} \quad (5)$$

where, ν is the Poisson's ratio of 0.3.

The *HEL* of the circular saw blades with different dynamic yield strengths can be calculated by Eq. 5. The material of circular saw blade is not fixed and concrete in the analysis below. Strength of circular saw blade body is characterized by dynamic yield strength. The dynamic yield strength is changed and HEL also follows change, according to Eq. 5, which is mainly used to analyze the calculation results according to the research findings of Ballard *et al.* (1990), as shown below.

As shown in Fig. 9, when the dynamic yield strength and the thickness of the circular saw blade were different, the equivalent radial stresses all increased first and then decreased with the peak pressure of the laser shock wave. The optimal peak pressure of the laser shock wave corresponded to the extreme value of the equivalent radial stress, marked by a circle as shown in Fig. 9. When the plastic deformation in the impact zone of the circular saw blade appeared saturated, the extreme value of the equivalent radial stress appeared. At this point, the equivalent radial stress decreases when the peak pressure of the laser shock wave continues to improve. The result can be explained according to the research of Ballard *et al.* (1990). Ballard pointed out that the maximum residual compressive stress on the surface of the impact zone can be obtained when the peak pressure of the laser shock wave is between 2 *HEL* and 2.5 *HEL* (Ballard *et al.*1990). When the maximum residual compressive stress on the surface of the impact zone appeared, the extreme value of the equivalent radial stress was also approximately present. Take Fig. 9 (a) as an example, σ_y^D =1000 MPa, and *HEL* corresponding to σ_y^D is 1750 MPa, according to Eq. 5. The extreme value of equivalent radial stress appeared when peak pressure of the laser shock wave was between 4 GPa and 5 GPa.

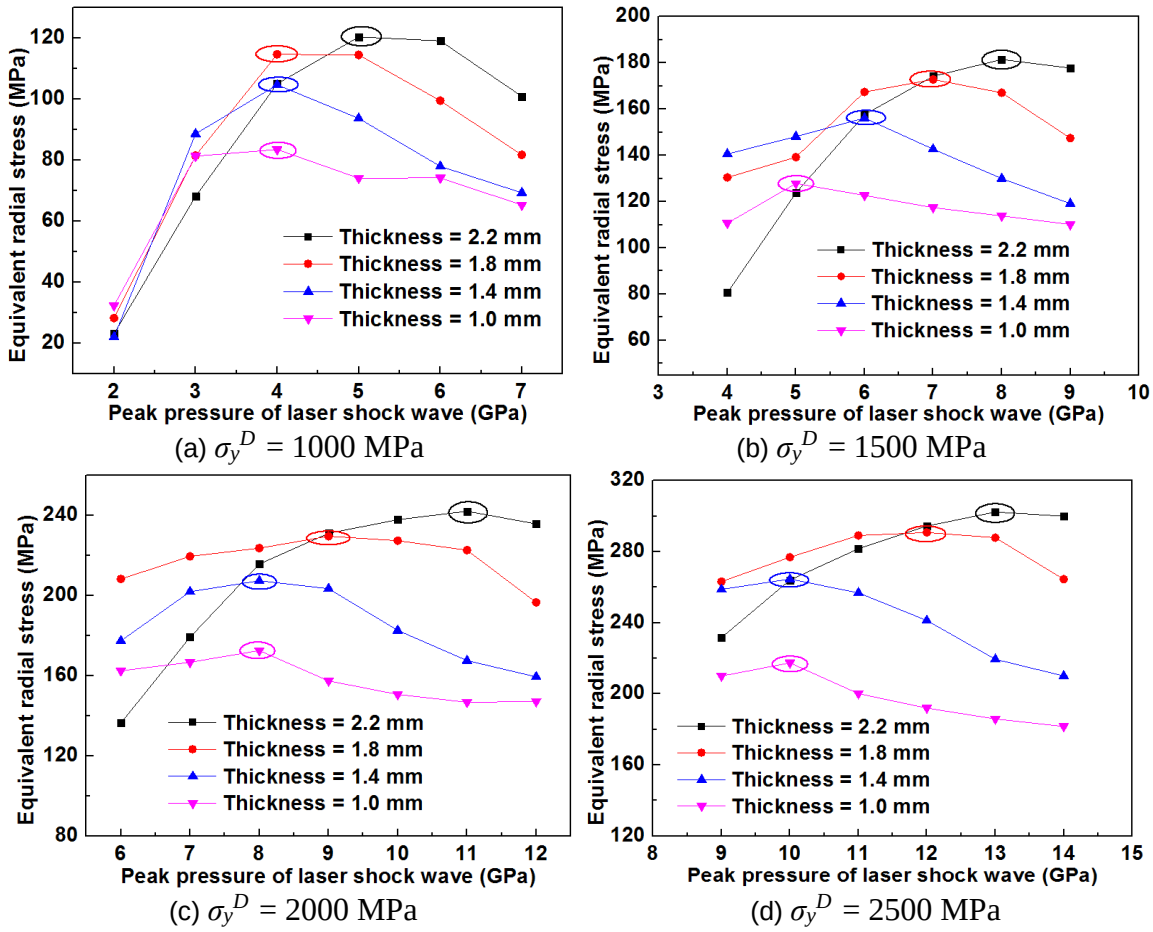

Fig. 9. Relationship between the equivalent radial stress and the peak pressure of the laser shock wave

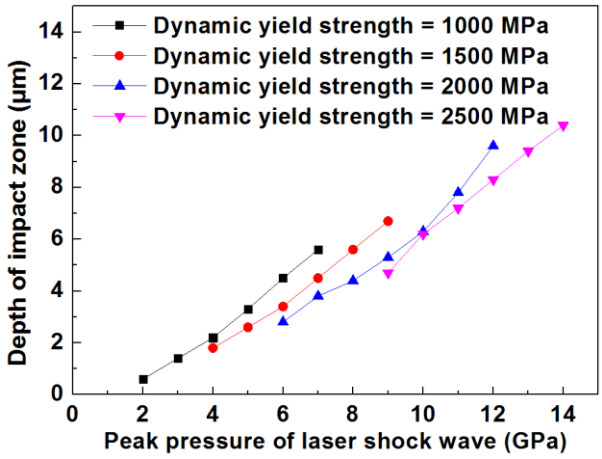

Fig. 10. Relationship between the depth of impact zone and peak pressure of laser shock wave

As shown in Fig. 10, the depth of impact zone was increased with peak pressure of laser shock wave. When dynamic yield strength of circular saw blade was increased, it needed a larger laser shock wave peak pressure to form a depth of magnitude for impact zone.

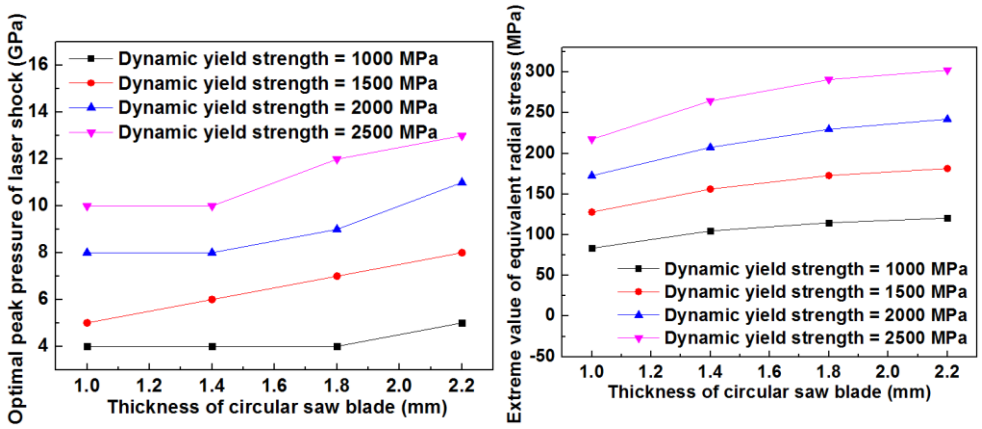

(a) Optimal peak pressure of the laser shock (b) Extreme value of the equivalent radial stress

Fig. 11. Optimal peak pressure of the laser shock and the extreme value of the equivalent radial stress under different dynamic yield strengths and thicknesses

As shown in Fig. 11, when the dynamic yield strength and thickness of the circular saw blades were different, the optimal peak pressure of the laser shock wave and extreme value of the equivalent radial stress were all different.

The optimal peak pressure of the laser shock wave increased with the thickness of the circular saw blade because the plastic deformation saturation state in the impact zone of thinner circular saw blades was more likely to occur under a smaller peak pressure. The optimal peak pressure of the laser shock wave increased with dynamic yield strength because the increase of deformation resistance increased the difficulty of plastic deformation. The optimal peak pressures of the laser shock wave were all close to the range of 2 *HEL* to 2.5 *HEL*.

According to the results in Fig. 8, the optimal peak pressure of the laser shock wave that corresponds to the extreme value of the equivalent radial stress can lead to the extreme value of the average tangential tensile stress at the outer edge of the circular saw blade. The extreme value of the equivalent radial stress noticeably increased with the dynamic yield strength of the circular saw blade. Thus, the extreme value of the average tangential tensile stress at the outer edge of the circular saw blade also increased with the dynamic yield strength. The room for tensioning effect improvement of the laser shock tensioning process widened with the increase of the dynamic yield strength of the circular saw blade.

CONCLUSIONS

1. Based on the mechanism of the laser shock tensioning process of a circular saw blade, a simplified model for the laser shock tensioning process was built *via* a finite element method and some reasonable assumptions. The model was shown to be correct by the experimental results. The laser shock tensioning process proved effective in improving the stability of circular saw blades.
2. The dynamic yield strength of circular saw blades had a great effect on the tensioning effect. There is an optimal peak pressure of the laser shock wave that can lead to the extreme value of the average tangential tensile stress at the outer edge of circular saw blades. It noticeably increased with the dynamic yield strength of circular saw blades.

3. The extreme value of the average tangential tensile stress at the outer edges of circular saw blades considerably increased with the dynamic yield strength, thus illustrating that the circular saw blade with a higher dynamic yield strength can obtain greater room for improvement of the tensioning effect.

ACKNOWLEDGMENTS

The authors gratefully acknowledge the financial support of the National Natural Science Foundation of China (No. 31600458) and the Fundamental Research Funds for the Central Nonprofit Research Institution of CAF (No. CAFYBB2017SY039).

REFERENCES CITED

Achintha, M., Nowell, D., Fufari, D., Sackeet, E. E., and Bache, M. R. (2014). "Fatigue behavior of geometric features subjected to laser shock peening: Experiments and modeling," *International Journal of Fatigue* 62, 171-179. DOI: 10.1016/j.ijfatigue.2013.04.016

Ballard, P., Fournier, J., Devaux, D., and Fabbro, R. (1990). "Study of the effects of a plastic wave induced by laser pulse in a metallic material. Application to the improvement of fatigue strength," *Proceedings of the American Mathematical Society* 17(5), 1140-1145.

Braisted, W., and Brockman, R. (1999). "Finite element simulation of laser shock peening," *International Journal of Fatigue* 21(7), 719-724. DOI: 10.1016/S0142-1123(99)00035-3

Cuellar, S. D., Hill, M. R., DeWald, A. T., and Rankin, J. E. (2012). "Residual stress and fatigue life in laser shock peened open hole samples," *International Journal of Fatigue* 44, 8-13. DOI: 10.1016/j.ijfatigue.2012.06.011

Dai, F. Z., Lu, J. Z., Zhang, Y. K., et al. (2014). "Effect of laser spot size on the residual stress field of pure Al treated by laser shock processing: Simulations," *Applied Surface Science* 316(1), 477-483. DOI: 10.1016/j.apsusc.2014.07.166

Ding, K., and Ye, L. (2006). "Simulation of multiple laser shock peening of a 35CD4 steel alloy," *Journal of Materials Processing Technology* 178(1-3), 162-169. DOI: 10.1016/j.jmatprotec.2006.03.170

Heisel, U., Stehle, T., and Ghassem, H. (2014). "A simulation model for analysis of roll tensioning of circular saw blade," *Advanced Materials Research* 1018, 57-66. DOI: 10.4028/www.scientific.net/AMR.1018.57

Huang, S., Zhou, J. Z., Sheng, J., Luo, K. Y., Lu, J. Z., Xu, Z. C., Meng, X. K., Dai, L., Zuo, L. D., Ruan, H. Y., *et al.* (2013). "Effects of laser peening with different coverage areas on fatigue crack growth properties of 6061-T6 aluminum alloy," *International Journal of Fatigue* 47(2), 292-299. DOI: 10.1016/j.ijfatigue.2012.09.010

Hfaiedh, N., Peyre, P., Song, H., Popa, I., Ji, V., and Vignal, V. (2015). "Finite element analysis of laser shock peening of 2050-T8 aluminum alloy," *International Journal of Fatigue* 70, 480-489. DOI: 10.1016/j.ijfatigue.2014.05.015

Hu, Y., Yao, Z., and Hu, J. (2006). "3-D FEM simulation of laser shock processing," *Surface and Coatings Technology* 201(3-4), 1426-1435. DOI: 10.1016/j.surfcoat.2006.02.018

Hua, D., Yun, W., and Lan, C. (2010). "Laser shock forming of aluminum sheet: Finite element analysis and experimental study," *Applied Surface Science* 256(6), 1703-1707. DOI: 10.1016/j.apsusc.2009.09.098

Li, B., Zhang, Z. K., Li, W. G., and Peng, X. R. (2015a). "Model for tangential tensioning stress in the edge of circular saw blades tensioned by multi-spot pressure," *BioResources* 10(2), 3798-3810. DOI: 10.15376/biores.10.2.3798-3810

Li, B., Zhang, Z. K., Li, W. G., and Peng, X. R. (2015b). "Effect of yield strength of a circular saw blade on the multi-spot pressure tensioning process," *BioResources* 10(4), 7501-7510. DOI: 10.15376/biores.10.4.7501-7510

Li, B., and Zhang, Z. K. (2017). "Research on the effect of yield strength of circular saw blade on roll tensioning process," *Journal of Wood Science* 63(2), 140-146. DOI: 10.1007/s10086-016-1602-3

Li, S., Wang, C., Zheng, L., Wang, Y., Xu, X., and Feng, D. (2016). "Dynamic stability of cemented carbide circular saw blades for woodcutting," *Journal of Materials Processing Technology* 238, 108-123. DOI: 10.1016/j.jmatprotec.2016.07.018

Luo, K., Lin, T., Dai, F. Z., Luo, X. M., and Lu, J. Z. (2015). "Effects of overlapping rate on the uniformities of surface profile of LY2 Al alloy during massive laser shock peening impacts," *Surface and Coatings Technology* 266, 49-56. DOI: 10.1016/j.surfcoat.2015.02.017

Nicoletti, N., Fendeleur, D., Nilly, L., and Renner, M. (1996). "Using finite elements to model circular saw roll tensioning," *Holz als Roh-und Werkstoff* 54(2), 99-104. DOI: 10.1007/s001070050146

Peyre, P., Fabbro, R., Merrien, P., and Lieurade, H. P. (1996). "Laser shock processing of aluminium alloys, application to high cycle fatigue behaviour," *Materials Science and Engineering: A* 210, 102-113. DOI: 10.1016/0921-5093(95)10084-9

Schajer, G. S., and Mote, Jr., C. D. (1983). "Analysis of roll tensioning and its influence on circular saw stability," *Wood Science and Technology* 17(4), 287-302. DOI: 10.1007/BF00349916

Schajer, G. S., and Mote, Jr., C. D. (1984). "Analysis of optimal roll tensioning for circular saw stability," *Wood and Fiber Science* 16(3), 323-338.

Szymani, R., and Mote, Jr., C. D. (1974). "A review of residual stresses and tensioning in circular saws," *Wood Science and Technology* 8(2), 148-161. DOI: 10.1007/BF00351369

Szymani, R., and Mote, Jr., C. D. (1979). "Theoretical and experimental analysis of circular saw tensioning," *Wood Science and Technology* 13(3), 211-237. DOI: 10.1007/BF00350225

Umetsu, J. (1989). "Confirmation of φ splitting in the distribution of residual stress in tensioning circular saws," *Journal of the Japan Wood Research Society* 35(9), 856-858.

Umetsu, J., Noguchi, M., and Matsumoto, I. (1994). "Measuring residual stresses in tensioned circular saws using x-rays," *Journal of the Japan Wood Research Society* 40(3), 268-273.

Article submitted: August, 29, 2017; Peer review completed: October 19, 2017;
Accepted: October 23, 2017; Published: October 25, 2017.
DOI: 10.15376/biores.12.4.9313-9325